Chapter 4

Redox Mediation through Integrating Chain Extenders in Active Ionomer Polyurethane Hard Segments in CdS Quantum Dot Sensitized Solar Cell

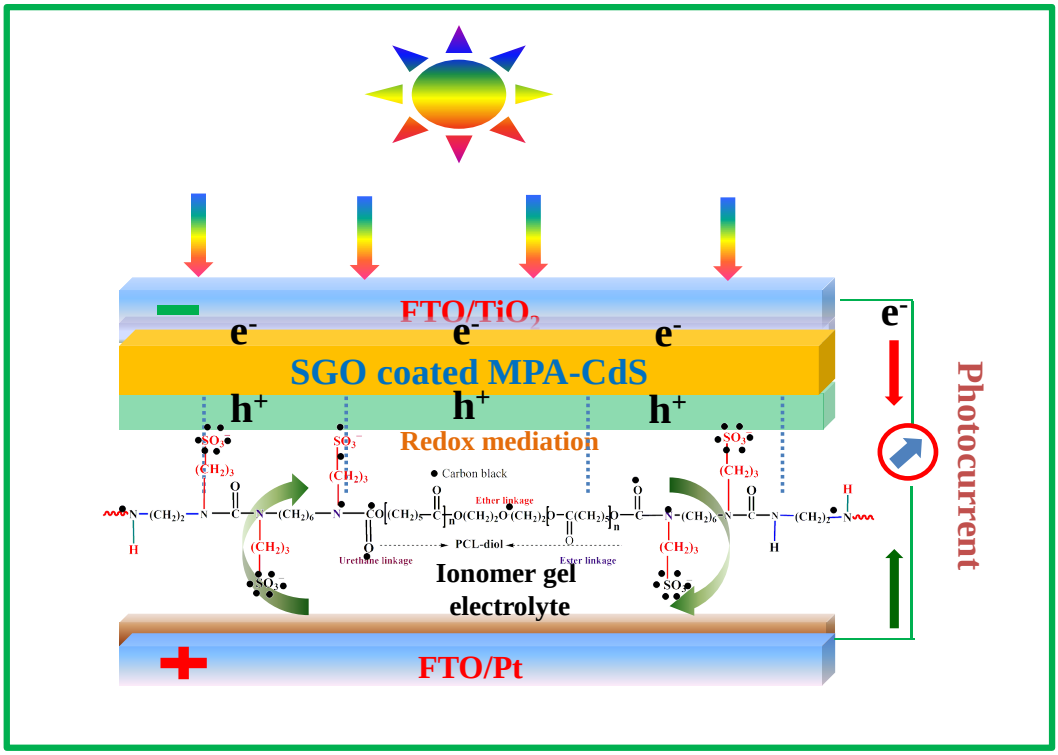

4.1. Introduction

Quantum dots sensitized solar cell has been emerged as highly efficient third-generation solar cell devices because their various opto-electronic properties make them well suited for photovoltaic applications [142]. Electrolyte structure is crucial component which can tune the open circuit potential and solar energy conversion efficiency of solar cell. The polymer electrolytes have favorable mechanical properties, ease of fabrication of thin films of desirable sizes, and an ability to form effective electrode–electrolyte contacts[143]. Most of the researchers have concentrated on designing novel polymer electrolytes possessing high ionic conductivity, good mechanical properties, and thermal stability for technological applications[144]. Recently, thermoplastic gel polymer electrolytes (TPGE) have been used in dye sensitized solar cell [145]. The TPGE exhibits thermoplastic behavior (i.e., the gel and sol states can be reversibly interconverted with a change in temperature. Polyurethane (PU) ionomers are a relatively new class of special polyurethanes which contain associated ionic centers at different chain intervals. A good polymer host for GPE should possess polar functional group, fast segmental dynamic of polymer chain, low glass transition temperature (T_g), high molecular weight, hydrophilic, wide electrochemical window, and high degradation temperature [146]. Despite the high conversion efficiency of QDSSCs, photovoltaic devices that employ a liquid electrolyte have the potential for other problems, including leakage, volatility, flammability, and quantum dot corrosion. There have been many attempts to replace the electrolyte in solid-state sensitized solar cells with alternatives such as inorganic hole transport materials, organic p-type polymer hole transporting materials, polymer included redox coupled electrolyte, and nanocomposite gel electrolytes [147]. Highly efficient semiconductor-sensitized solar cells have been developed through chemical interaction [55]. Gel polymer electrolyte does not encounter leakage issue since the salt solution or tagged ionic group is fully entrapped within the polymer network structure.

Borghei et al. developed TEMPO-oxidised cellulose nanofiber (TOCNF) as electrolyte carrier for polysulfide aerogel with energy conversion efficiency of 0.52% in CdS QDs sensitized solar cell [148]. Yang et al. prepared PAAm-PANi supported polysulfide gel electrolyte for QDSS cell with conversion efficiency of 2.33% [68]. Yu et al. prepared polyacrylamide supported polysulfide hydrogel electrolyte for CdS/CdSe co-sensitized solar cell with a conversion efficiency of 4.0% [65]. Patel et al. developed polysulfide gel polymer electrolyte using 30 w% PEG (M_w = 4000) for QDSS cell. The device exhibited conversion efficiency of 4.09% [149]. Jin et al. developed graphene oxide tailored polyacrylamide (PAAm/GO) supported polysulfide composite gel electrolytes for QDSS cells with power conversion efficiency of 4.10% [66]. Polyurethanes possess many advantages including high flexibility, low temperature property, high tensile strength, excellent adhesion, improved rheological properties, good chemical, and abrasion resistance [150]. Polyurethanes have a hydrophobic nature. Ionic moieties are known as an internal emulsifier and polyurethane ionomers [114,151]. Ionic content is incorporated in polyurethane chain to develop redox active as well as semiconducting moiety. Because of interionic electrostatic forces, as well as the high degree of thermodynamic incompatibility between the ionic groups and the polymer matrix (typically nonpolar hydrocarbon) , these ionic groups tend to aggregate in the bulk material [152]. However, solvation (solvent uptake) reduces the extent of aggregation result in enhanced mobilization. Ionic conductivity varies with solvation capacity or electrolyte uptake. Polycaprolactone glycol (PCL) exhibited the best mechanical properties, presumably because of the hydrogen bonding by the ester groups and the high coulombic forces of the PU ionomers [153,154].

In this study, thermoplastic polyurethanes have been synthesized via variation of chain extender (diammine and diol based chain extending unit) and soft segment unit. A series of sulfonated PU ionomers were prepared by reacting urethane NH group of different

classical PUs with NaH and 1, 3-propane sultone in organic solvents. The chemical and electronic environment has been tuned around urethane linkage (-NHCOO-) to establish better electrochemical redox active sites. Soft segment has been modified with oxygenic functional group between hard segment and chain extending units of polyurethane ionomer. Electrical conduction and adhesion properties have been produced through hydrophilic properties of redox active pendant group across polyurethane chain. 3-mercaptopropeonic acid has been used to cap or stabilized the quantum size of CdS QDs. Quantum dot sensitized solar cells have been fabricated via integration of MPA caped CdS, interfacial dopants (PANi and SGO) and electrochemical redox active electrolyte. Redox mediation maintains excitons separation at the interface of QDs/electrolyte. Therefore, a series of redox active functionalized polyurethane ionomer gel have been developed to sustain continuous redox mediation in QDSS cells. Polyaniline has been employed to mobilize the interfaces (photoanode/PANi/ionomer electrolyte) which may enhance the extent of photovoltaic redox mediation. Sulfonated grapheme oxide has been used as interfacial dopants to reduce photoexcited charge recombination at the interface of photoanode/electrolyte. Electron rich charged SGO was employed to passivate the interfaces (photoanode/SGO/ionomer electrolyte) which reduce the extent of recombination on electrolyte surface. The redox active gel electrolytes were produced through size difference and electron repulsive environment around hard segment content in electrolyte structure. Interestingly, carbon black supported polyurethane composite ionomer gel electrolyte has been explored to intensify the redox meditative behaviour in pendant group across urethane linkage. QDSS cells have been characterized under photo illumination of 100 mW/cm^2 intensity of light. Photovoltaic measurement has revealed structural stability of gel matrix during the course of photo redox mediation.

4.2. Results and Discussion

4.2.1. Chain extension, structural variation and interaction of hydrophilic group in polyurethane chain

Syntheses and chemical structure of ether based polyurethanes through reaction of chain extenders with active NCO –terminated pre-polyurethane at 30% hard segment contents have been shown in **Figure 4.1(a), (b).** Ester based polyurethane has been synthesized via reaction of (HMDI+PCL-diol+EDA) to create multiple oxygenic functionalities. Interestingly, polyurethane ionomers have been developed via situ polymerization reaction of hard segments content with ϒ – propane sultone.

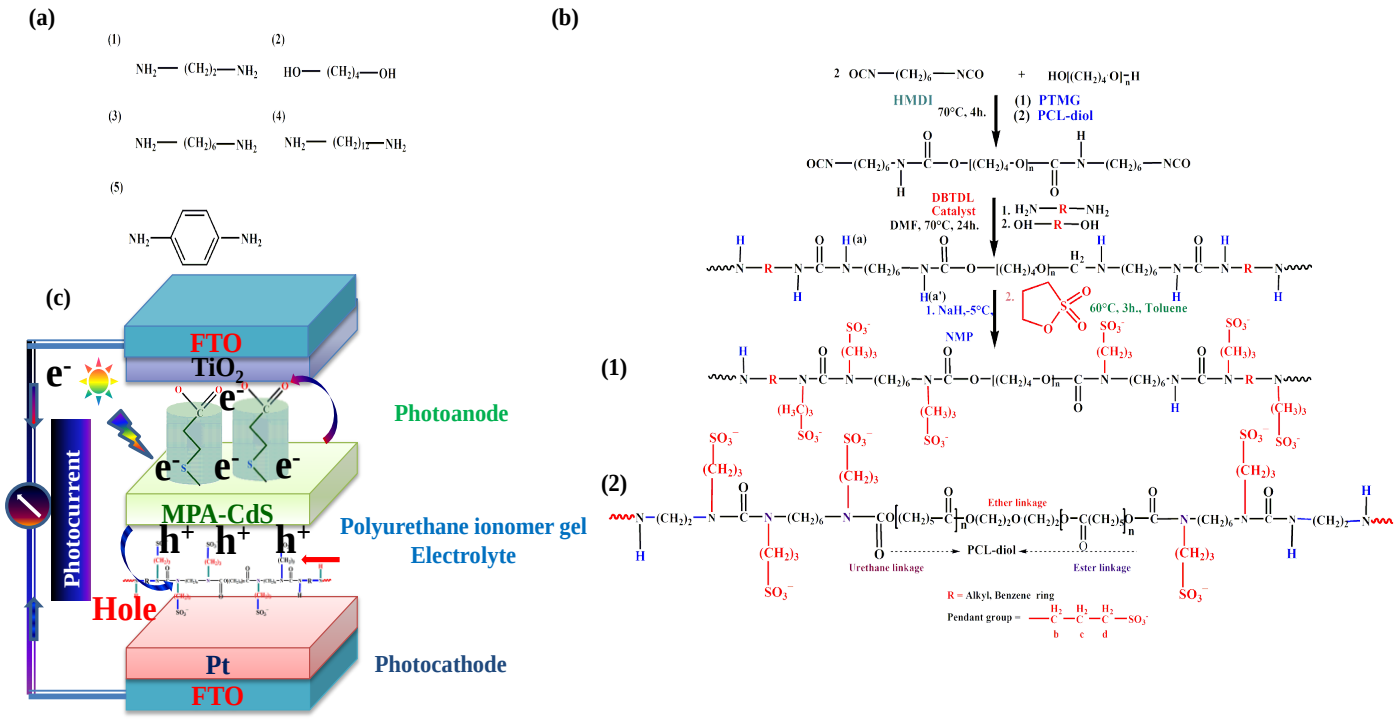

Scheme 4.1: (A) Chemical structure of chain extenders (1) EDA (2) BD (3) HDA (4) DDA (5) PDA. (B) Schematic representation of (a) Synthesis of ether based polyurethanes through variation of chain extenders and structural modification of hard segment contents in polymer chain (b) Synthesis of ester based polyurethane by maintain chain extending unit (EDA) constant. (C) Fabrication of QDSS cell through structural integration of components in layer design and indication of pathways for charge transport under photo illumination**.**

^{1}H NMR spectra characterized the presence of interactions at hard segment contents in polyurethane and its ionomeric chain. Non functionalized urethane linkage contains one

active hydrogen while functionalized urethane linkage has three set of protons (**Figure 4.2a**). The chemical shift measurement revealed that protons showed different values of chemical shift due to distinct chemical and electronic environment (**Figure 4.2b**). The butane-diol (BD) extended polyurethane showed chemical shift 7.04 ppm. The content HMDI protons (four CH_2) between two terminal isocyanate linkages exhibit chemical shift in the range of 1.20- 1.59 ppm. The other two $–CH_2$ proton attached with isocyanate –N moieties display its peak at 2.92 ppm. The functionalized polyurethane exhibits peak at 3.52 ppm which is attributed to $–SCH_2$ (2) (proton corresponds to pendant group attached to urethane linkage) which is found to be absent in pure PU-BD. The middle peak $–CH_2$ (3) and outer $–NCH_2$ (4) are exhibited at 3.28 and 1.64 ppm, respectably. Similarly, dodecyl diamine extended polyurethane exhibits a characteristic peaks at 7.0 and 7.95 ppm which are corresponding to the presence of two different –NH proton around urethane linkage (-NHCOO) and urea linkage (-NH-CO-NH-). The functionalized polyurethane (SPU–DDA) shows characteristic peaks at 8.42, 7.95 and 6.06 ppm which are assigned to the functionalized hard segment, non functionalized urea linkage (NHCOO) and $-OCH_2$ proton in polyurethane ionomer. The down field chemical shift of –NH proton is due to reduction of inter hard segmental hydrogen bonds in polyurethane ionomer. The outer $–SCH_2$ (2) peak appears at 3.57 ppm while middle $–CH_2$ (3) appears at 1.47 ppm, respectively [95]. Highly functionalized polyurethane ionomer showed intense peaks due to presence of more number of pendant protons in polyurethane chain.. The terminal nitrogen (urethane sites) linked $–CH_2$ proton showed chemical shift around $\delta = 1.64$ ppm. All these spectral data supports the interaction of ϒ-propane sultone and confirms the formation of polyurethane ionomer.

FTIR spectra show shifting of absorption peaks due to interactions of ionic species or segments with polyurethane chain. The FTIR data have been shown in **Table 4.1**.The absorption peaks at 3323 and 1534 cm^{-1} were attributed to stretching and bending vibrations

of N-H groups in urethane group of PU-BD. Ionomer matrix shows broad absorption band towards higher wavenumber which indicates interchains H-bonding is reduced upon interaction of ϒ-propane sultone (**Figure 4.1c** and **Figure 4.3a**). The absorption peaks at 1685, 1677 and 1721 cm^{-1} were due to the C=O groups in urethane groups of PU-BD, PU-DDA and ester groups of soft segments (PU-PCL-EDA). On other hand Ionomer matrix, the peaks at 1660, 1645 and 1664 cm^{-1} are due C=O groups of SPU-BD, SPU-DDA and SPU-PCL-EDA. As sodium cations interact strongly with both ether due to PTMG and the (C=O) of urethane linkage [155]. The strong interactions shifted absorption frequency towards lower wavenumber. The additional absorption peaks at 1183, 1174 and 1185 cm^{-2} are assigned due to symmetric vibrations of S=O group of anionic segments of polyurethane ionomer chain. These peaks are found to be absent in pristine polyurethanes

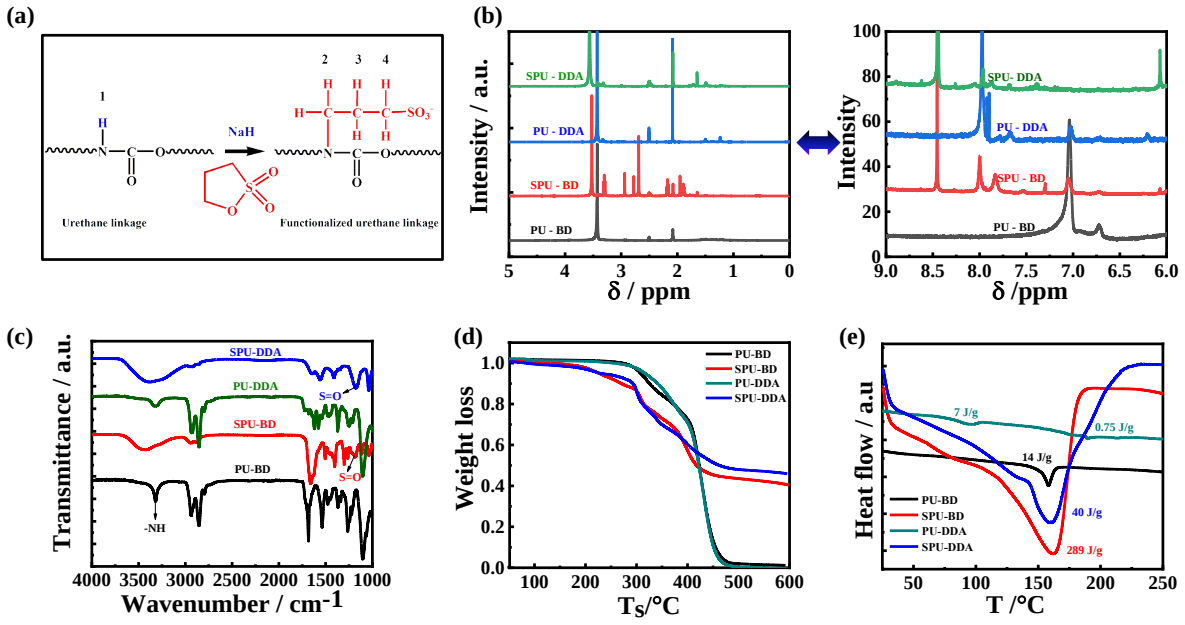

Figure 4.1: Structural content of urethane linkage and functionalized urethane linkage in polyurethane chain (b) Solution phase ^{1}H NMR spectra of short chain (BD) and long chain (DDA) extended polyurethanes and its ionomer matrix in solvent d_6-DMSO with their spectral peaks resolution in the range of chemical shift (δ = 0 - 9 ppm). (c) Solid thin film based FTIR spectra of short chain (BD) and long chain (DDA) extended polyurethanes and its ionomer matrix with spectral resolution of 4 cm^{-1}. (d) Thermogravimetric analysis (TGA) of short chain (BD) and long chain (DDA) extended polyurethanes and its ionomer matrix.

(e) Differential scanning calorimetry (DSC) 0f short chain (BD) and long chain (DDA) extended polyurethanes and its ionomer matrix in scanning temperature range of 25-250°C

Functional group	PU-BD	SPU-BD	PU-DDA	SPU-DDA	PU-PCL-EDA	SPU-PCL-EDA
N-H (Stretching)	3323	3437	3320	3390	3335	3437
C=O (s)	1685	1660	1677	1645	1721	1664
C-N (s)	1662	1633	1575	1557	1628	1563
N-H (Bending)	1534	1508	1540	1557	1536	1501
C-O-C (as)	1103	1114	1103	1100	1107	1112
S=O (s)	-	1183	-	1174	-	1185
S=O (as)	-	1220	-	1272	-	1264

Table 4.1: FTIR Wavenumber (cm^{-1}) of Polyurethanes and polyurethane ionomers

Figure 4.1d displays thermogram for structurally different PUs and functionalized polyurethanes (SPUs). The degradation temperature (5% weight loss) of different polyurethanes is analyzed over the temperature range of 40 – 600 °C. Polyurethane and its ionomer show multistage degradation due to decomposition of hard segments and soft segments [156]. The BD tagged PU (PU-BD) shows its first degradation at 299 °C and the SPU–BD starts degradation at 210 °C due to decomposition of functionalized hard segment contents. PU-DDA degrades at 303 °C while SPU-DDA started degradation at 215 °C. The first degradation for EDA and HDA extended PUs are observed at 340^{o} and 313 °C, respectively. The degradation index of hard segments in aliphatic EDA extended PU is observed at 243°C while its sulphonated segments degrade at 153°C. The degradation temperature for PDA extended PU slightly lowered down and is observed at 305 °C. The urethane groups (aromatic ring attached sites) undergo fast degradation which accounts for thermo-oxidative nature of urethane linkages. SPU–PDA ionomer shows thermal degradation at 90 °C which is assigned to the susceptible chain scission in the hard segmented zone and also observed second and third degradations (**Figure 4.2a**)**.** The chain extenders contribute to create differences in the density of hydrophilic and hydrophobic environment (segment). The PCL modified PU displays even lower degradation temperature (297 °C) due to the presence

of high oxygen content in soft segment (ester linkages) leading to the absorption of large amount of heat. The PCL modified sulfonated PU exhibits degradation behavior at 218 °C due to hydrophilic nature of polar groups (pendant group) over hard segments. The composite S(PU+CB)-PCL-EDA ionomer exhibits lower thermal degradation temperature (123 °C) which is accounted for the adsorption of carbon black (CB) over the surface of pendant group and thus supports its thermal stability **(Figure 4.3b).** The SPU-PCL-EDA ionomer exhibits greater stability and attributes to the compatibility of soft segments over the hard segments.

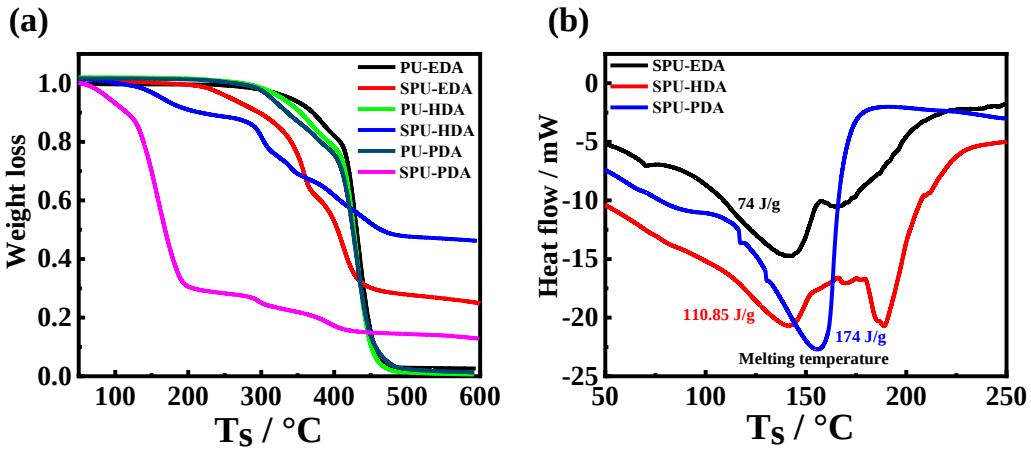

Figure 4.2: (a) Thermogravimetric analysis (thermal stability) for ether based polyurethane and its ionomer matrix under different chain extending units (structural variation of HSC). (b) DSC measurements of polyurethane ionomers under different hard segment content due to integration of chain extenders

The DSC thermograms of polyurethane and sulfonated polyurethane ionomer matrix have been characterized with well-defined exotherms and sharp melting temperature. The glass transition (T_g), enthalpy of melting (ΔH_m) and melting temperature (T_m) varies with functionalization density on hard segment contents [157]. **Figure 4.1e** shows thermal transitions in polyurethane and polyurethane ionomer matrix. Pristine PU-BD exhibited sharp melting behavior due to melting of polar hard segment contents [158]. The melting peak was observed at T_m = 158°C and ΔH_m = 14 J/g. The T_g and T_m were observed around 87°C and 161°C for SPU-BD ionomer matrix. The PU-DDA chain exhibited characteristic melting

behavior at T_m = 189°C and ΔH_m = 0.75 J/g due to presence of long chain hard segment contents. The SPU-DDA showed T_g = 130°C, T_m = 161°C and ΔH_m = 71 J/g. The melting of sulfonated long chain hard segment content was observed at lower temperature than the pristine PU-DDA. This is probably due to ion–ion interaction (ionic repulsion) in long chain coiled structure. The thermo characteristic T_g = 71°C, T_m = 142°C and ΔH_m = 74 J/g were obtained for SPU-EDA which indicates strong interactions between anionic pendant and urethane –NH groups. While SPU-HDA ionomer showed T_g = 80°C, T_m = 140°C and ΔH_m = 110 J/g. The SPU – PDA ionomer exhibits T_g = 89°C, T_m = 155°C and ΔH_m = 174 J/g because of presence of aromatic surface which indicates large heat absorption than SPU-EDA ionomer (**Figure 4.2 b**). Similarly PU-PCL-EDA showed characteristic T_m = 247 °C and ΔH_m = 0.36 J/g (**Figure 4.3c**). The soft segment modified polyurethane ionomer (SPU-PCL-EDA) matrix exhibited T_m =162 °C, ΔH_m = 120 J/g . The carbon black (CB) dispersed composite polyurethane ionomer S(PU+CB)-PCL-EDA exhibited T_g = 125 °C, T_m= 192 °C and ΔH_m = 239 J/g **(Figure 4.3d)**. The CB dispersed thermogram shows high crystalline content than the crystallinity of SPU-PCL-EDA. This is probably high adsorption of CB on Sulfonate group of hard segment leading to shifting of melting behavior towards higher melting temperature [159,160].

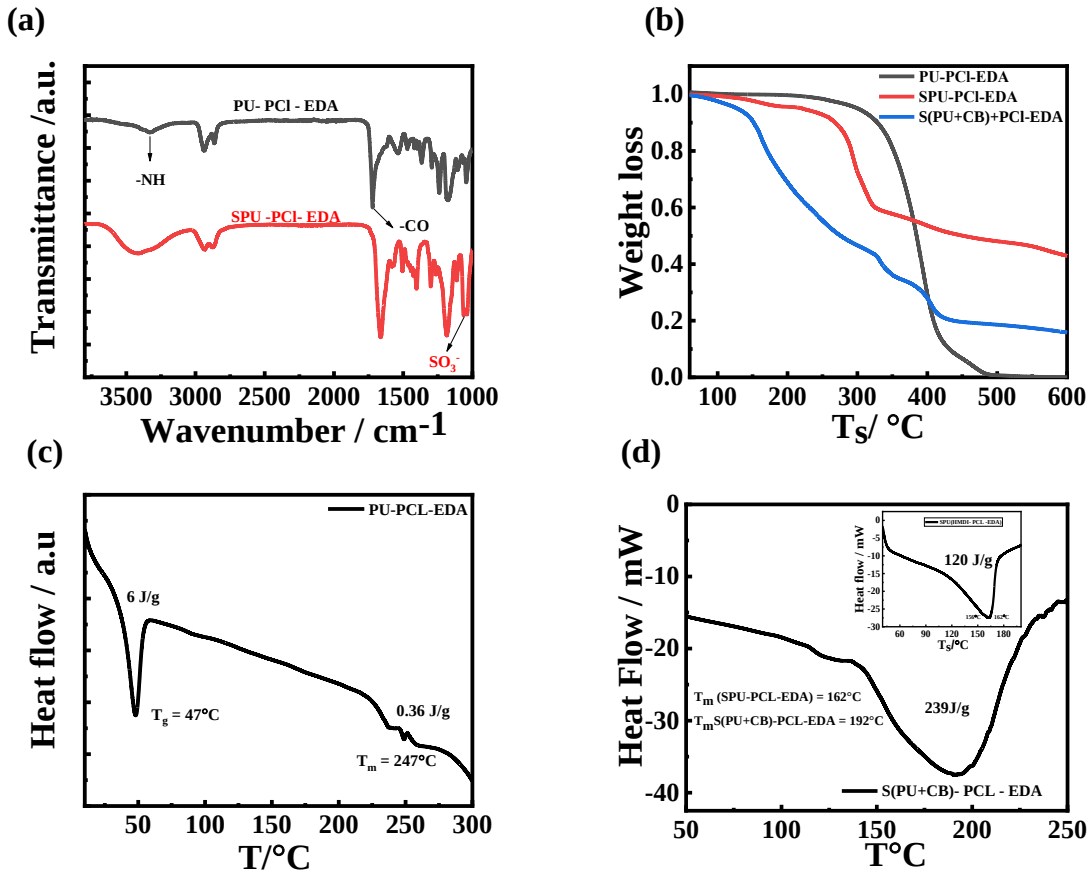

Figure 4.3: (a) Solid state FTIR spectra of ester (PCL-diol) based polyurethane and its ionomer matrix. (b) Thermogravimetric analysis of ester based polyurethane, ionomer matrix and composite ionomer matrix.(c) DSC measurements of synthesized ester based polyurethane. (d) DSC measurements of ionomer matrix and composite ionomer matrix.

Figure 4.4a represents the absorption spectra of structurally modified polyurethanes (PU-BD, SPU-BD, PU-DDA and SPU-DDA) with their characteristic transition peaks. The polyurethanes are enabled to display π - π* and n - π* electronic transitions with the absorption of UV-visible light. The increased chain length (C_4- diol to C_{12}- diammine) of polyurethane shifted the absorption band or edge towards longer wavelength. The PU-BD shows a characteristic absorption peak at 215 nm ($\pi \rightarrow \pi^*$) and maximum absorption peak at 285 nm due to ($n \rightarrow \pi^*$) transition in urethane carbonyl group. The PU-DDA showed characteristic absorption maxima 212 nm and 295 nm due to greater interaction of long chain hard segment content. The SPU-BD displayed absorption peak at 221 nm and 296 nm which

confirmed the presence of chromophoric group (pendant group) in polyurethane chain. The SPU-DDA exhibited characteristic absorption peaks at 222 nm and 306 nm. The large bathochromic shift is assigned with more interaction of ϒ-propane sultone across urethane linkage of PU-DDA. **Figure 4.4c** presents the UV-visible absorption spectra of PU-EDA, SPU-EDA, PU-HDA, SPU-HDA and PU-PDA and SPU-PDA. The absorption peaks at 220 and 255 nm are attributed to PU-EDA while SPU-EDA showed maximum absorption peaks at 224 nm and 278 nm. The SPU-HDA showed characteristic absorption (n-π*) at 303 nm which is greater than absorption peak (291 nm) for PU-HDA. The p-phenylenediamine extended polyurethane showed the absorption peak 209 nm and 281 nm due to urethane structure and one additional broad peak at 529 nm appeared probably due to presence of conjugated aromatic ring. The sulfonated polyurethane (SPU-PDA) ionomer exhibited absorption band at 222 nm and 304 nm and additional peak blue shifted because of reduction of conjugation upon interaction with pendant group. Similarly, maximum absorption peak transition (n-π*) were observed at 300 and 288 nm for SPU-PCL-EDA and S (PU+CB)-PCL-EDA against 292 nm in pristine PU-PCL-EDA. Carbon black passivate the absorption behaviour of functionalized urethane linkage leading to shifting of absorption band towards blue side of spectrum.

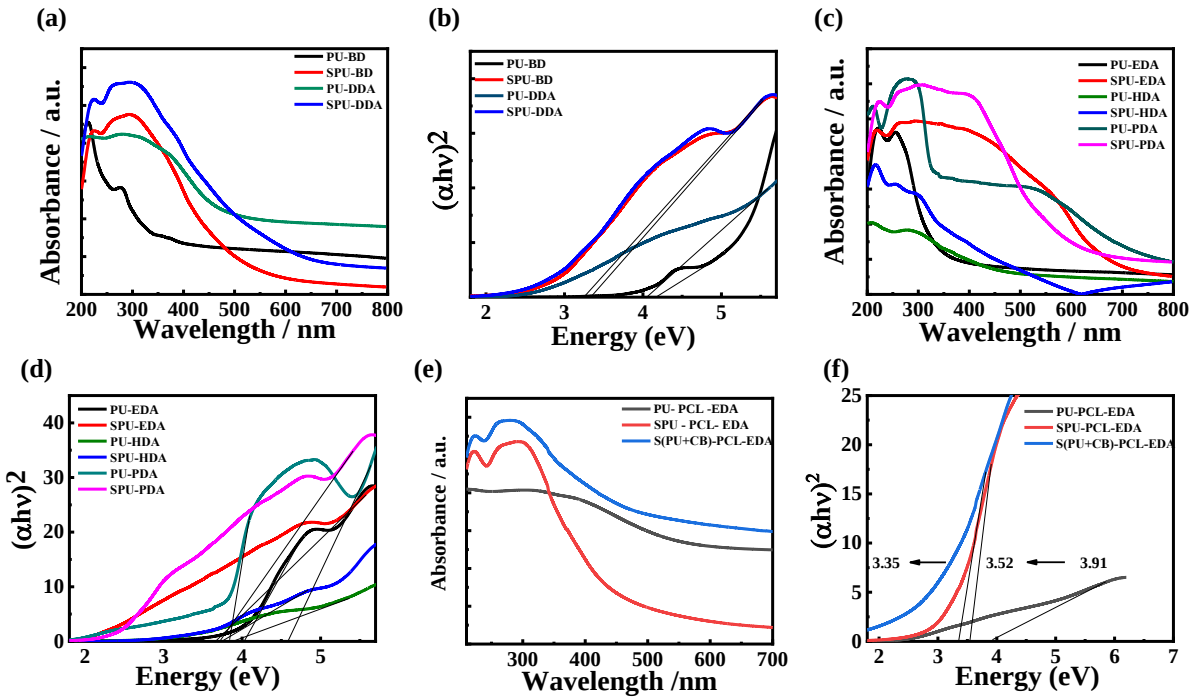

Figure 4.4 (a) Solid state UV-visible absorption spectra of short chain (BD) and long chain (DDA) extended polyurethanes and its ionomer matrix. (b) $(\alpha h\upsilon)^2$ vs. hυ plots for estimation of energy gap from absorption edge of obtained spectra. (c) UV-visible absorption spectra of polyurethanes and its ionomer matrix under different chain structure. (d) Tauc's plots of absorption spectra to estimate energy gap from absorption edge**. (**e) UV-visible absorption spectra of PU-PCL-EDA, SPU-PCL-EDA and S (PU+CB+EDA). (f) Tauc's plot

The Tauc's plot in **Figure 4.2b, c** shows the representative extrapolation and intersection on x-axis corresponds to band or energy gap originated from absorption edge of pristine polyurethanes and its ionomers. The direct energy gaps are calculated as 4.01, 4.34, 3.91, 3.85, 4.06 eV for PU-EDA, PU-BD, PU-HDA, PU-PDA and PU-DDA respectively. Further, energy gap of 3.77, 3.39, 3.54, 3.65 and 3.30 eV are calculated from absorption edge of SPU-EDA, SPU-BD, SPU-HDA, SPU-PDA and SPU-DDA, respectively. The energy gaps of 3.91, 3.52 and 3.35 eV are estimated for PU-PCL-EDA, SPU-PCL-EDA, composite ionomer through soft segment variation on polyurethane chain **(Figure 4.4f).**

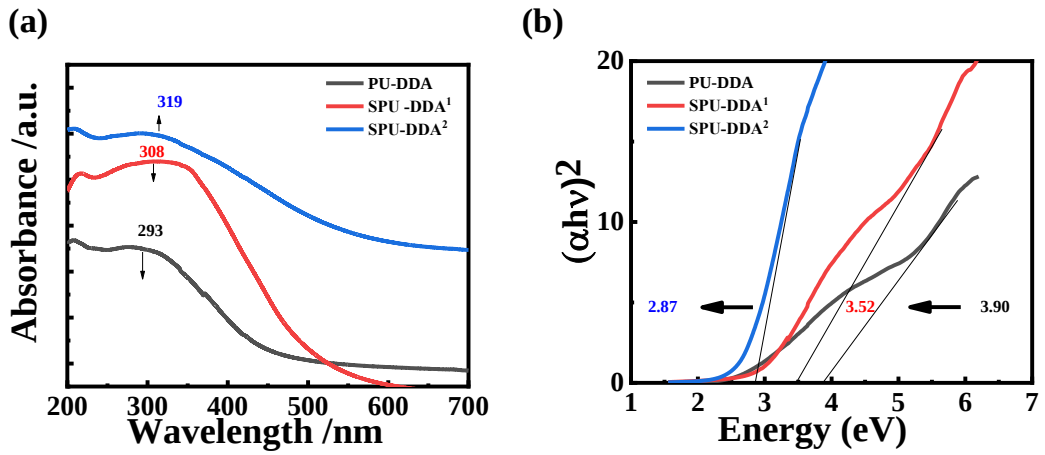

Figure 4.5: (a) Effect on absorption spectra of PU-DDA with variation of weight ratio of sulfonating agent (ratio of weight of NaH to weight of ϒ- propane sultone). (b) Tau's plot to estimate energy gap.

Polyurethane ionomer shows structural quantum confinement which can be observed clearly in the absorption spectra of SPU-DDA as a function or weight ratio of sulfonating agents (**Figure 4.4a**). Pristine PU-DDA shows absorption peak at 293 nm due to n-π* transition. The SPU-DDA shows red shifted absorption band at 308 nm at a weight ratio of 0.17 of sulfonating agent. Moreover, absorption peak red shifted as the weight ratio of sulfonating agents increased from 0.17 to 0.36. The shifted band shows absorption peak at 318 nm which confirms the extent of interactions of sulfonating agents with polyurethane hard segments increases and thus absorption edge become more diffused or wider with high concentration of sulfonating agents. The shifting of band gaps has been shown in **Figure 4.4b.**

4.2.2. Electrochemical properties of electrolyte responsive component in PU ionomers

The potential of the working electrode was swept in the range of −2 V– 2 V, with a scan rate of 20 mV s^{-1}. Pristine polyurethane PU-BD does not show any oxidation or reduction peak or phase transition [161]. However, little broader peaks appeared either side of oxidation or reduction due to mass transfer, structural relaxation or oxygen release from urethane linkage. On the other hand sulfonated polyurethane ionomer exhibited positive oxidation and negative

reduction potential because of presence of characteristic sharp anodic peak and cathodic peak, respectively. The oxidation-reduction process is reversible. The BD extended SPU ionomer shows its characteristic onset edge potential at 0.697 V because of presence of electron delocalization on oxygenic functional surface of chain extender linkage (BD). The long chain DDA extended SPU exhibits a characteristic onset oxidation edge at 0.721 V against 0.12V in pristine PU-DDA. It can be attributed to the separation of functional hard segment over long chain of the polyurethane results in enhancement of surface energy. The oxidation edge potentials 0.707 V and 0.711 V are observed for SPU-EDA and SPU-HDA, respectively. The PDA linked SPU shows its oxidation edge at 0.717 V which is compromisingly little larger than SPU-EDA and demonstrates some extent of stabilization of sulfonate group with π electron cloud of the benzene ring surface. The SPU-PCL-EDA shows its onset edge potential at 0.683 V due to change of soft segment which affects the functional hard segments and improve chain segmental motion as a whole. The composite ionomer S(PU+CB)-PCL-EDA (carbon black composite) has lowest oxidation potential value at 0.600 V which is attributed to the assistance of carbon black to enhance the ease of charge transfer pathway and oxidation of adsorbed functional group. Thus, CV measurements revealed direct evidence of absence of electroactive center in polyurethane chain.

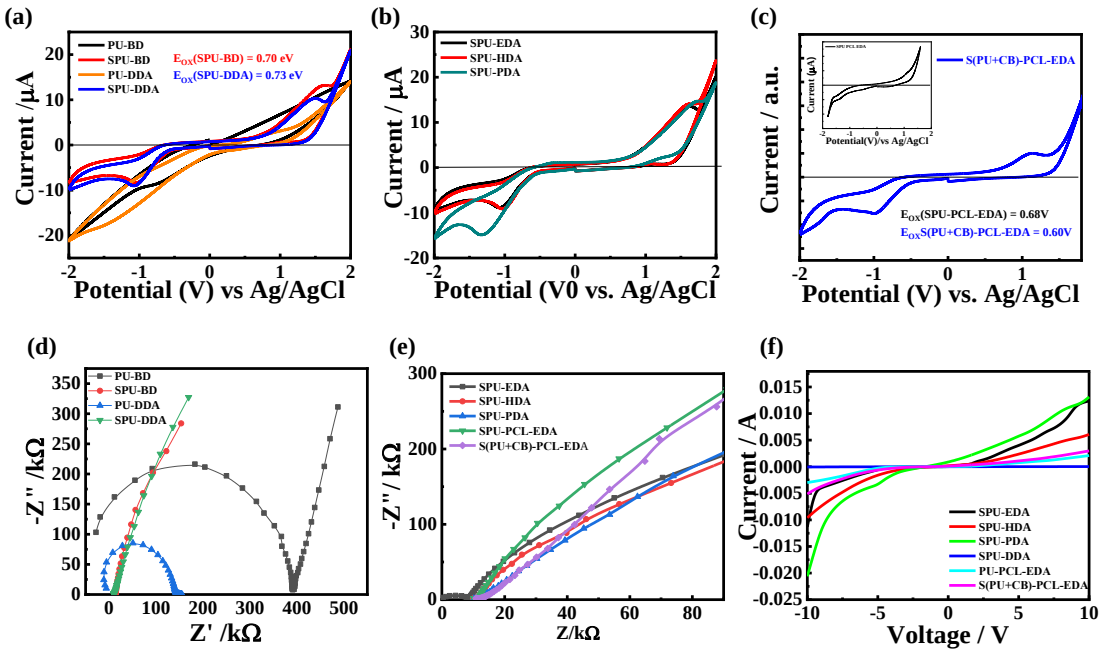

Figure 4.6: (a) Solution phase cyclic voltammetry measurements of short chain (BD) and long chain (DDA) extended polyurethanes and its ionomer matrix with a scan rate of 20 mV/s operated at room temperature. (b) Solution phase cyclic voltammetry measurement for different ionomer electrolyte (influence of chain structure on redox properties). (c) Cyclic voltammetry characterization of ionomer electrolyte in pristine and composite phase (influence of functional group on redox properties (d) Electrochemical impedance spectroscopy measurements in solution phase of polyurethanes (PU-BD and PU-DDA) and its ionomer matrix for the estimation of electrical (ionic) conductivity at room temperature. (e) EIS measurement and influence of chain structure on ionic conductivity of polyurethane ionomers. (f) I-V characteristic measurements of ionomer gel as thin film on FTO (electronic conductivity measurements)

Electrocatalytic activity of redox active ionomer electrolytes			
Polyurethane ionomer electrolyte	**P_{AE}(V)**	**P_{CE}(V)**	**$E_{PP} = P_{AE} - P_{CE}$**
SPU-EDA	0.707	-0.563	1.270
SPU-BD	0.697	-0.582	1.279
SPU-HDA	0.711	-0.621	1.332
SPU-DDA	0.727	-0.611	1.338
SPU-PDA	0.717	-0.582	1.299
S(PU+CB)-PCL-EDA	0.600	-0.493	1.093
SPU-PCL-EDA	0.683	-0.850	1.533

Table 4.2: Electrocatalytic redox reaction in ionomer segment at the interface of different ionomer electrolyte/counter electrode (Pt)

Electrocatalytic activity of active ionomeric segments in polyurethane chain can be understood by peak to peak onset separation potentials in electrochemical voltammetry. The minimum peak to peak separation is a measure of fast reversible reaction on ionomeric

segments. The Peak to peak separation potentials are enlisted in **Table 4.2** for different ionomeric structures. Composite ionomer possess lowest peak to peak separation potential. It is probably due to preferential adsorption of carbon black on ionomeric segments which facilitate fast charge transport at the interface of ionomer electrolyte/Pt.

Ionic conductivity depends on volume of redox active ionic segments in polyurethane chain. Segmental motion varies with mean free volume of ionomeric segments. Ionic conductivity is due to preferential adsorption of Na^+ from sulfonating agent onto polar surface of polyurethane ionomers. The EIS plots for ionic conductivities of functionalized polyurethane ionomer electrolytes having different chain extenders are shown in **Figure 4.6d, e**. Pristine PU-BD and PU-DDA exhibited ionic conductivity around 7.63×10^{-6} and 2×10^{-5} S/cm. The ionic conductivities of 5.07×10^{-5} and 2.2×10^{-5} S/cm are calculated through charge transfer resistance in solution of SPU-BD and SPU-DDA ionomer, respectively. The long chain extended SPU-DDA does not have sufficient conductivity and lower value is due to ionic aggregation in coiled structure. Aggregation lowers the surface area leads to decrease ionic conductivity [162]. The ionic conductivity was calculated 4.0×10^{-4} S/cm due to perfect semicircle region. The other semicircle drawn through spikes curve exhibited the ionic conductivities of 5.5×10^{-5} and 2.2×10^{-5} S/cm and are assigned for SPU-HDA, SPU-PDA, respectively. The side chain (pendant group) probably helps to improve the ionic conductivity of ionomer electrolyte. Ion conduction is due to segmental motion of pendant group as well as polyurethane chain. The aromatic ring and long chain extender causes higher interaction leads to the formation of coiled or shrinkage structure. The variation of soft segment (PTMG to PCL) in the polyurethane ionomer controls the conductivity value of 1.6×10^{-5} S/cm. The composite S (PU+CB)-PCL-EDA ionomer exhibits the conductivity of 6.3×10^{-5} S/cm, showing slightly increasing tendency in the composite ionomer. This is attributed to the adsorption of carbon black (CB) on the polar surface as well as ionic pendant

group of the urethane linkage. Carbon black reforms conducting nanochannel on the surface of redox active group. Thus, ionic conductivity varies with ionic content and hard segment content in polyurethane chain.

Polyurethane ionomer matrix	Electronic conductivity (S/cm)
SPU-EDA	1.8
SPU-HDA	14.4×10^{-3}
SPU-PDA	2.9
SPU-DDA	3.8×10^{-4}
SPU-PCL-EDA	0.48
S (PU+CB)-PCL-EDA	0.71

Table 4.3: electronic conductivity of polyurethane ionomers developed as thin film over the surface of FTO

The calculated ionic conductivity of polyurethane ionomers film has been shown in **Table 4.3**. The I-V characteristic curves have been shown in **Figure 4.6f.** The electronic conductivity is calculated around 1.8 S/cm for EDA extended SPU ionomer at a 0.09 mm film thickness while 14.4×10^{-3} S/cm and 3.8×10^{-4} S/cm for HDA and DDA extended SPU under same experimental condition. It is evident that conductivity is reduced as the length of chain extender increases which is due to the enhancement of electrostatic repulsion of charge located on surface of functional group in coiled or aggregated structure. The electronic conductivity is found to be improved in case of p – phenylenediamine extended sulfonated chain because of participation of nonbonding electron available on –N atom of the chain towards aromatic ring in conjugation with π electrons. Conjugation improves delocalization of charge on ionomer surface. The overall resonance of ionic charge integrated with the mobility of ring electrons result in exhibition of $\sigma_{electronic}$ = 2.9 S/cm for SPU-PDA ionomer. The PCL improves the property of soft segment in EDA extended SPU by exhibiting π resonance with covalently attached –O- atom nearby same carbon atom of chain and conductivity is evaluated around 0.48 S/cm. The composite ionomer S(PU+CB)-PCL-EDA

exhibits 0.71 S/cm as electronic conductivity. Carbon black improves electronic conduction because of synergistic behavior on the surface of CB adsorbed pendant group. Structural variation influences the electronic conductivity [163]. The ionomer structures having delocalized and resonating content, are more susceptible to transport electrons [164]. Moreover, high hydrophilicity of sulfonate group, the electron conduction is affected with time of environmental saturation on functionalized anionic fragments.

4.3. MPA functionalized CdS QDs and quantum confinement effect on stabilized structure

F**igure 4.7a** represents the UV–vis absorption spectra of free CdS and MPA-capped CdS nanoparticles at different concentration of surface capping agent (MPA) measured at room temperature. Free CdS shows broad band absorption and transition. The absorption peak for all the samples were observed to be blue shifted as compared to that of bulk CdS (515 nm) [165]. The UV-visible absorption spectra demonstrate that two separate absorption peaks; one due to linked carboxylate $–COO^-$ (surface chromophore) and the second one for thiol coordinated CdS particle. The extent of blue shift varies with concentration of covalently linked capping moieties on core CdS surface. The chromophoric thiol ion captures the surface of CdS particles and thereby prevents the nucleation/agglomeration. The maximum absorption peaks (λ_{max} = 467, 458, 452, 438, 444 nm) were recorded at a series of lower concentration (0.45, 0.65, 0.70, 0.80 and 1.0 M) of capping agent. The higher concentration (1M) is more prone to enable red shifting in absorption band due to surface agglomeration and coagulation of negatively charged capping agent. The direct band gaps of 2.65, 2.71, 2.74, 2.83 and 2.79 eV are estimated through Tauc's plot **(Figure 4.7b)** and the optimized band gap of 2.71 eV is revealed as highly efficient because of proper balance between capping agent and CdS particle. However, high concentration capping agent causes interionic repulsion on the surface of CdS nanoparticles leads to aggregation of particles.

Hence, quantum confinement is due to reduction of size of the particle which tends to stabilization of VB structure. Band gap increases with decrease in particle size.

TEM image of MPA capped CdS (E_g = 2.71eV) has been shown in **Figure 4.7c.** Image shows clear formation of spherical particles which are distributed in the size range of 12-15 nm. The size resembles little larger than the size range of quantum dots. Size expansion can be explained by the photocatalytic oxidation of the thiol (-SH) groups on the surface of the quantum dots. The oxidized thiol forms disulfides, which in turn lowers the binding efficiency to the surface of CdS particle. The 3-mercaptopropeonic acid functionalizes the surface of QDs and stabilize CdS as a negatively charge particle ($-COO^-$) at basic pH. Thin film absorption spectra of electron transport layer (Ti-nanooxide) and photoanode has been shown in **Figure 4.7d.** Titanium oxide absorbs UV light (357 nm) with intense absorption peak. However, CdS adsorbed Ti-nanooxide film shows broad band transition confirming red shifted spectra. Photoanode is susceptible to harvest visible portion of spectrum.

Quantum confinement creates discontinuous surface states due to quantized electronic behaviour. Quantum states affect the electrochemical activity of CdS particle. Cyclic voltammetry measurements of capped CdS particles has been shown in **Figure 4.7e**

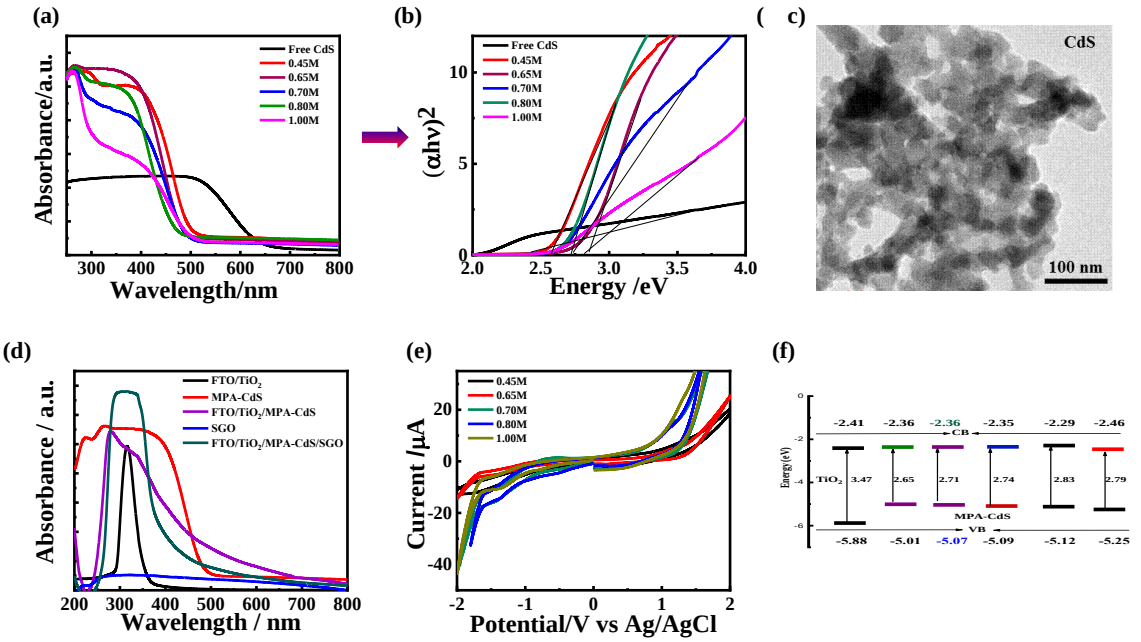

Figure 4.7: (a) Solid state UV-visible absorption spectra of free CdS and MPA caped CdS particles under variation of concentration of MPA molecule. (b) Tauc's plot to estimate band gaps from absorption edge. (c) TEM image of MPA caped CdS nanoparticles. (d) UV-visible absorption spectra of thin film Ti – nanooxide (photocatalyst) photosensitizer, SGO and multi layered structure to characterize photo harvesting properties. (e) Solution phase CV measurements of caped CdS particles to investigate redox properties. (f) Energy levels and band diagram for different CdS nanoparticles.

4.4. Functionalized graphene oxide and extent of surface functionalities

Functionalization confirms the high surface activity of S-GO sheets, which are able to reduce the interfacial tension more effectively than GO. Interfacial interaction interaction energy is due to the presence of different functional groups and multiple adsorption sites. UV-visible absorption spectra shows broad peak at 323 nm which confirms the presence of new chromophore on GO surface (**Figure 4.6d**). The SGO nanosheets showed wavy and well exfoliated layered structure resulting from hydrophilic environment of pendant group grafted on the GO surface. The surface structure maintained the layer structure as shown in TEM image of **Figure 4.8a**

Figure 4.8b shows the FT-IR spectra of GO and its modified form (S-GO). The adsorption bands corresponding to the C=O carbonyl stretching at 1,728 cm^{-1}, the O–H

deformation vibration at 1,379 cm^{-1}, and the C–O stretching at 1,065 cm^{-1}. Besides the ubiquitous O–H stretches which appear at 3,451 cm^{-1} as a broad and intense signal, the resonance at 1595 cm^{-1} can be assigned to the vibrations of the adsorbed water molecules but may also contain components from the skeletal vibrations of un-oxidized graphitic domains [166]. All of these confirmed that the graphite was oxidised and functional groups were introduced onto the GO sheets. The peak at 1193 cm^{-1}, confirm the presence of a sulfonate group which appears absent in the spectra of GO. Specifically, GO needs modification to develop desirable functional properties such as adhesion and dispersion.

Interlayer d spacing is inversely proportional to the diffraction angle. The diffraction peak observed for GO sheet is broader compared to that of more densely distributed crystalline peak in SGO. **Figure 4.8c** compares the XRD patterns of the GO and SGO samples. In the case of GO, a sharp peak, which corresponds to the (001) plane, appears at 11.09° while SGO shows most intense crystalline peak at 22.92°. The positive shifting of diffraction angle confirming that the sulfonation of GO is prone to occur on the edge of GO and in between the layers of GO. Moreover, XRD pattern also shows many crystalline peaks around most intense crystalline peaks. Stack size decreases as the level of sulfonation increases [167]. The reduced stack size facilitates fast charge transport due to short distance.

Cyclic voltammetry clearly shows onset oxidation at 0.29V in dispersed phase solution (**Figure 4.8d**). However, sulfonated Graphene oxide (SGO) shows shifting in onset oxidation towards lower value (0.12V) which confirms that ionic pendant group lowers the surface energy due to enhanced inter-repulsion of ionic moieties on flat surface. Electrochemical impedance spectroscopy clearly reveals that incorporation of alkyl pendant group reduced the solution phase charge transport resistance compared to GO and MPA-CdS (**Figure 4.8e)**. The conductivity values were obtained as 4.72×10^{-5}, 7.7×10^{-5} and $6.26 \times$

10^{-4} S/cm for MPA-CdS, GO and SGO, respectively. Hydrophilic pendant group improves electrical (ionic) conductivity of functionalized surface of graphene oxide.

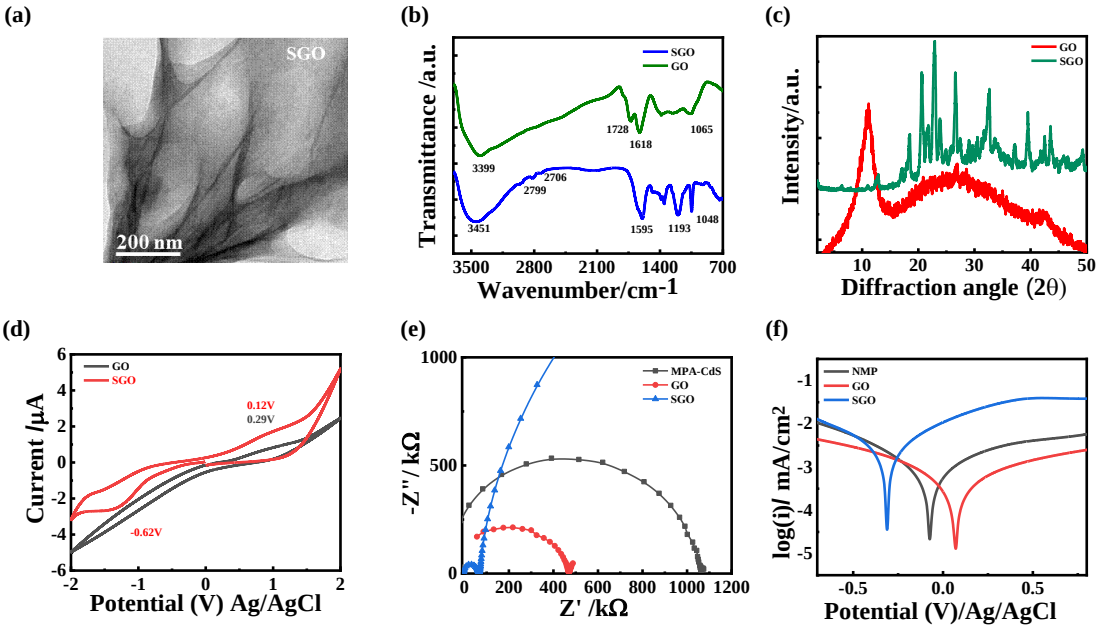

Figure 4.8: (a) TEM image of sulfonated graphene oxide (b) Solid state FTIR spectra of GO and SGO. (c) XRD measurements of GO and SGO (d) CV measurements of GO and SGO (e) ESI measurements for GO, SGO and MPA caped CdS QDs. (F) electrocatalytic and corrosion behaviour of SGO with reference to GO.

The attached sulfonate group shifted Ecorr towards lower value (negative potential) as compare to the level of Ecorr in GO confirming SGO behaves as non corrosive material either on the surface of QDs or ionomer electrolyte. The shifting of Ecorr has been shown in **Figure 4.8f**.

4.5. Electron lifetime studies and control of recombination center in polyurethane ionomers

Frequency response analysis was carried out in solution phase to estimate Bode plots for the measurement of lifetime of free electron on the surface of redox active units The lifetime of free electrons is calculated as 25.4, 63.2, 51, 61.7 and 78 ms for SPU-EDA, SPU-BD, SPU-HDA, SPU-PDA and SPU-DDA ionomer, respectively (**Figure 4.9a**). The curve depicts that SPU-HDA and SPU-DDA have one additional maximum peak points which were attributed

to delocalized trap states and thus responsible for probable recombination. Similarly, The free electron lifetime on SPU-PCL-EDA and composite ionomer S(PU+CB)-PCL-EDA are evaluated as 51 ms and 77 ms, respectively **(Figure 4.9b)**. Life time composed of chemical capacitance and recombination resistance on the surface of redox active group.

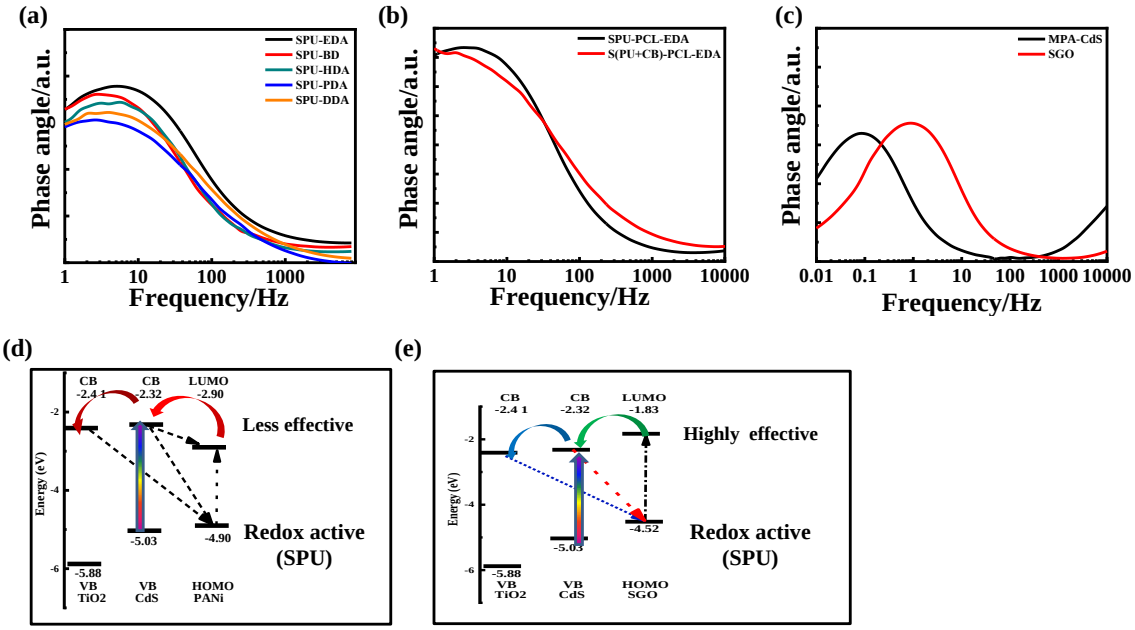

Figure 4.9 Bode plot for ionomer electrolyte in solution phase (a) influence on free electron lifetime measurement on the surface of active group of different chain extended ionomer electrolyte (b) influence on lifetime with oxygenic functionalities in pristine and composite ionomer structure. (c) Bode plots for QDs and SGO in solution phase. (d) Charge transport and recombination –activation on PANi coated CdS photoanode. (e) Charge transport and recombinations on SGO coated photoanode sensitized device.

In a similar fashion, Bode plot demonstrates that the lifetime values 1.75 s and 189 ms are obtained for solution state pristine MPA-CdS and SGO, respectively (**Figure 4.9c**). The higher lifetimes are attributed to high charge transfer resistance on the surface of QDs. However, surface defects or traps are charge recombination centers [168]. Therefore, interfacial interaction can lower the lifetime value in QDSS cells. Thus, it can increase the probability of charge recombination at the interface.

When photoanode comes in contact with ionomer electrolyte. Interfacial energy differences facilitate electron hole pair separation in QDs. In general, surface defects promote

the recombination reaction in the trap states. The possible charge recombination pathways have been shown in **Figure 4.9d, e.** The LUMO energy levels of PANi are slightly lower than the energy level of CB of QDs. Charge recombination and its activation might be slower at the interface. On other hand, the LUMO level of SGO is slightly above to that of CB of QDs. Electrons can be reactivated at the interface efficiently.

4.6. Fabrication scheme and interfacial alignment of energy levels in QDSS cell

Charge transport is due to energy difference at the interface of two layers. The positive oxidation potential shifted HOMO towards deeper value in ionomer matrix. Systematic energy levels have been shown in **Scheme 4.2a**. Although, all ionomeric HOMOs level are located slightly deeper with respect to E_{VB} of Quantum dots. The energy levels of LUMOs of all ionomeric gel situated above to that of E_{CB} of QDs. The optimum tuned Quantum dots possess (E_{VB} = -5.03eV, E_{CB} = -2.32eV). The E_{CB} CdS (QDs) is located above to that of E_{CB} of TiO_2. Photosensitization generates electron-hole pair. Interfacial energy difference drives the charge for photovoltaic reaction and continuous light harvesting [169]. Photoexcited electron can be injected into CB of TiO_2 and photoexcited hole towards redox active group in ionomer electrolyte during photovoltaic reaction (**Scheme 4.2b**). The oxidized ionomer electrolyte is electrocatalysed on active sites of Pt counter electrode. A thin layer of SGO has been inserted at the interface of photoanode/ionomer electrolyte to improve electrical properties synergistically. The SGO also prevents charge recombination and thus works as passivation layer

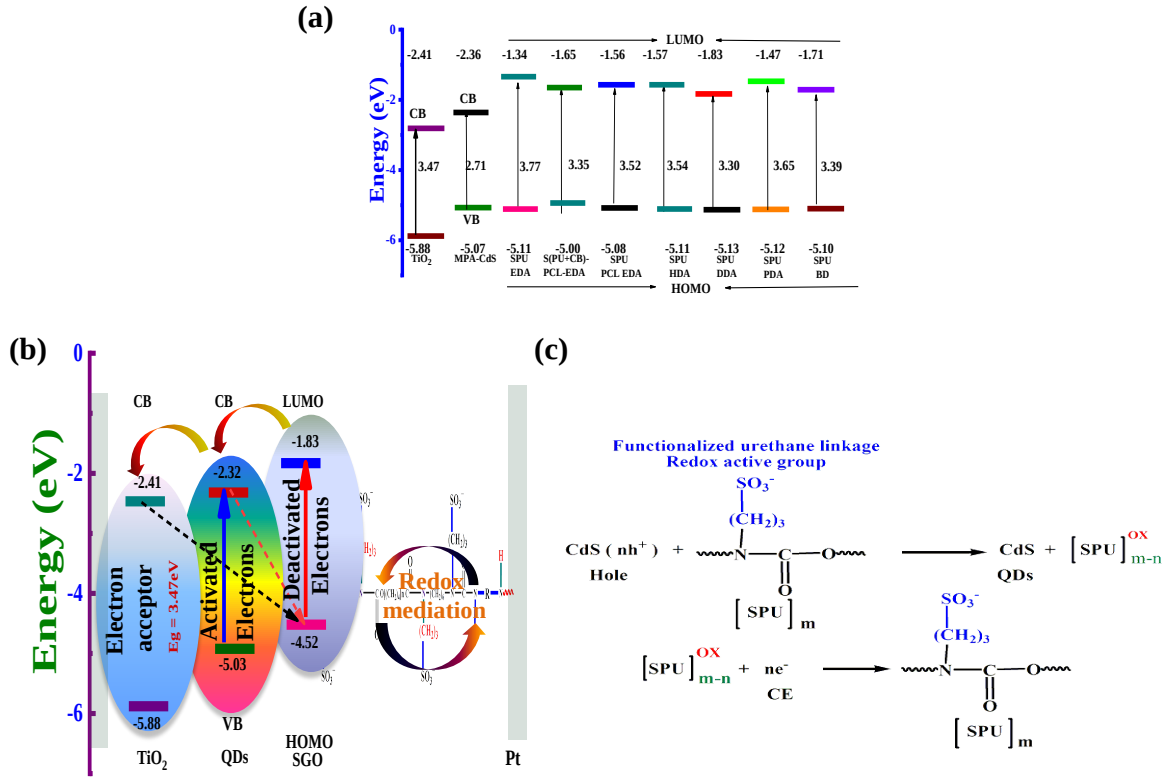

Scheme 4.2: **(a)** Systematic representations of energy level, band diagram and its interfacial alignment. (b) Charge transport and recombination pathways at the interface photoanode/ionomer electrolyte/counter electrode. (c) Possible functional mechanism (photovoltaic reaction) of ionomer electrolyte with QDs and counter electrode.

Polyurethane ionomer electrolyte possesses functionalized hard segment contents. The diamine chain extenders create functionalized urethane and urea linkage in ionomer matrix while Di-ol chain extender generates functionalized urethane linkage in ionomer matrix. Since each linkage contains redox active units. The redox properties might be slightly differs at different linkages of active ionomeric group. However, functionalized urethane ionomer content facilitates photovoltaic redox process due to lower surface energy. The $[SPU]_m$ consisted of redox active ionomer group having total 'm' number of pendant group over the hard segments (**Scheme 4.2c**). Under photovoltaic illuminations, some redox active units (n) will be oxidized to catalyze the photo generated hole on the surface of QDs and

itself is converted into $[SPU]^{ox}_{m-n}$ phase which consequently reduced on counter electrode by accepting ne^- to maintain the reversibility of electrolytic function.

4.7. Photovoltaic properties of Quantum dot sensitized solar cell

4.7.1. Influence of different ionomer gel electrolyte for photovoltaic reaction in QDSS cell

Photovoltaic devices are designed as layered structure. Device has been developed as sandwich type assembly of photoanode, ionomer electrolyte and counter electrode (**Figure 4.8a**). In general, open circuit potential defines redox properties of electrolyte in device during photovoltaic reaction.

The fabricated QDSS cell with SPU-EDA ionomer gel showed photovoltaic characteristic values (J_{SC} = 1.58 mA/cm^2, V_{OC} = 0.38V; η = 0.03%). Photovoltaic efficiency is low probably because of insufficient charge transport across active ionomer group leading to high interfacial charge transfer resistance which accelerates recombination of photoexcited electron with hole either in QDs or oxidized ionomer. On other hand, same ionomer gel exhibited photovoltaic characteristic (J_{SC} = 1.17 mAcm^{-2}, V_{OC} = 0.40V; η = 0.16%) with PANi coated photoanode sensitized device. Similarly, ionomer gel shifted photovoltaic values (J_{SC} = 1.34, V_{OC} = 0.42V; η = 0.23%) with SGO coated photoanode sensitized device. The little improvement in V_{OC} was observed in SGO coated device than PANi coated QDSS cell. This is attributed to passivation of charge recombination from negatively charged environment and oxygenic functionalities on SGO surface. The little enhancement of photocurrent density in SGO coated device is due to synergistic absorption of light on SGO which may additionally inject towards CB of QDs and TiO_2.The probable retardation of charge recombination in SGO coated device is due to presence of shallow LUMO energy levels than PANi LUMO levels. The QDSS cell exhibited photovoltaic characteristic values (J_{SC} = 1.03 mAcm^{-2}, V_{OC} = 0.45V; η = 0.12%) with SPU-HDA ionomer gel when inserted

directly at the interface of non coated CdS sensitized photoanode and counter electrode. The further improvement of V_{OC} is attributed to efficient charge transport across expanded distribution of alkyl sulfonate group in SPU-HDA chain. The ionomeric content can reduce the extent of aggregation in SPU-HDA than SPU-EDA. The PANi coated photoanode sensitized device exhibited improvement in photocurrent and efficiency because of possible enhancement of extent of photoexcited electron injection through conducting interconnected channel at PANi/ ionomer gel interface. The low V_{OC} (0.36V) is probably due to interfacial hole accumulation which may slows down the redox process in ionomer electrolyte [170]. But SPU-HDA exhibits little improvement in SGO coated photoanode sensitized device. The device showed comparable V_{OC} to that of non coated photoanode sensitized device. This is likely due to improvement of hole exchange process at the interfaces of SGO coated photoanode/ionomer gel/counter electrode.

On other hand, SPU-PDA exhibited photovoltaic characteristic values (J_{SC} = 2.73 $mAcm^{-2}$, V_{OC} = 0.49V; η = 0.35%) in non coated photoanode sensitized device .The V_{OC} value is observed to be increased which may be possible acceleration of redox process in ionomer electrolyte. The expanded π cloud in p-phenylenediamine ring is responsible to prevent the extent of charge recombination or back reaction towards ionomer electrolyte [171]. In similar hand, PANi coated photoanode sensitized device showed little demotion in V_{OC} which may be explained on the basis of interfacial aggregation due to interaction of benzene rings on PANi and SPU-PDA ionomer. However, SGO coated photoanode sensitized device showed improved photocurrent density (2.51 $mAcm^{-2}$) and open circuit potential (0.52V). The efficient photovoltaic reaction is due to synergistic enhancement of interfacial electrical property which may increase the charge transport process with sufficient reversible change in ionomer electrolyte.

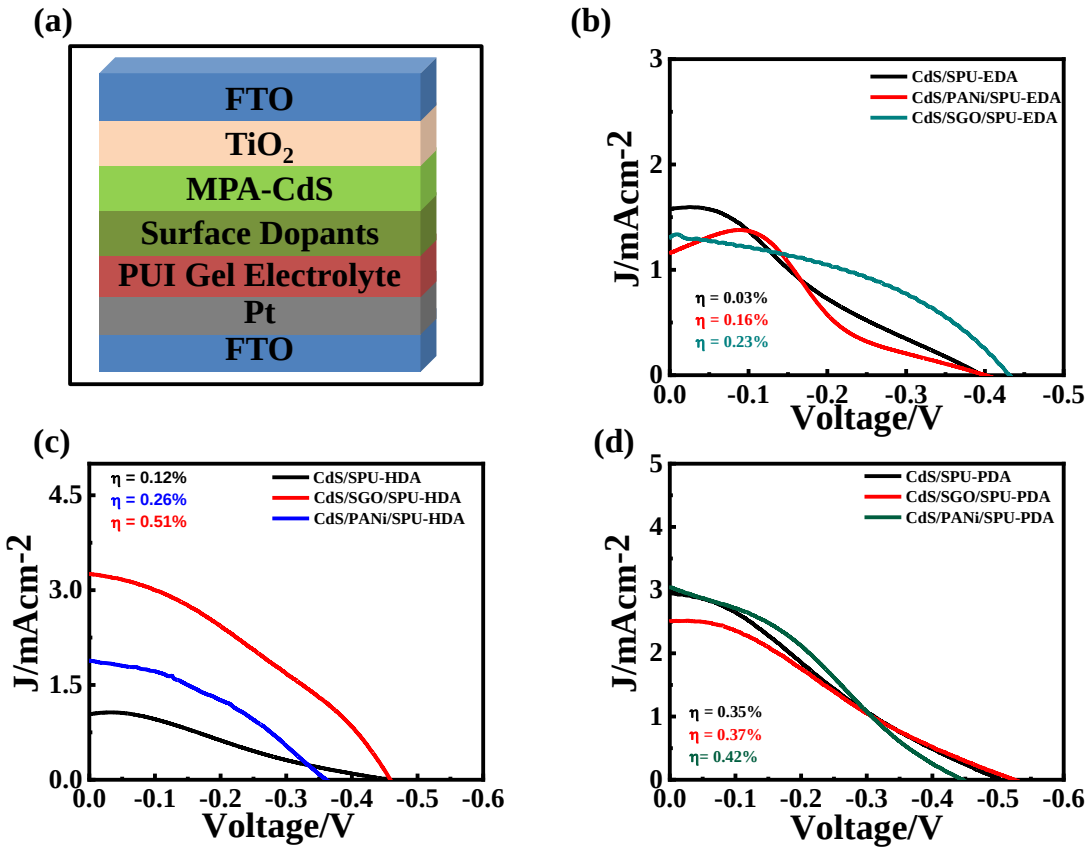

Figure 4.10: (a) Coated Layered structure of fabricated device. (b) J-V characteristic measurements of QDSS cells using SPU-EDA ionomer electrolyte on different interfaces of photoanode.(c) J-V curves QDSS cells with SPU-HDA ionomer electrolyte (d) J-V curve of QDSS cells using SPU-PDA ionomer electrolyte. Each Ionomer gel electrolyte 30% (w/v)

4.7.2. Variation of chain length and functionality in ionomer electrolyte structure

Charge transport is hindered across cross linked or aggregated structure in gel electrolyte. Quantum dot sensitized solar device exhibited photovoltaic values (J_{SC} = 0.42 mA/cm^2, V_{OC} = 0.52V; η = 0.04%) with non coated CdS photoanode sensitized system. On other hand, SPU-DDA showed photovoltaic reaction with photocurrent density of 0.50 mA/cm^2 and low open circuit potential of 0.31V. In farmer case saturation current density is not obtained as standard characteristic. However second one showed solar characteristic curve with low open circuit potential. The long chain ionomer gel is more susceptible towards chain aggregation which may delay the redox process in ionomeric content. But SPU-BD showed efficient photovoltaic effect (J_{SC} = 3.37 mA/cm$^{2;}$ η = 0.66%) with good solar characteristic curve in

SGO coated photoanode sensitized device. The enhanced performance is due to reduced charge recombination in ionomer electrolyte. Photocurrent density increases due to possible alignment of CB of TiO_2 towards downward at the interface. SPU-DDA ionomer electrolyte improves photocurrent density ($1.37mA/cm^2$) but further lowers open circuit potential (0.27V). The photovoltaic conversion efficiency is achieved little high which may be due to synergistic absorption of light by QDs as well SGO layer. SGO facilitates activation of the deactivated electron which intensifies number density of injected electron in CB of Ti - nanooxide consequently increases the photocurrent density.

Highly sulfonated ionomer gel (SPU-EDA) showed abnormal solar to light conversion efficiency (0.57%) in SGO coated photoanode sensitized device. Photocurrent density drops sharply from steady state. This can be explained on the basis of more surface defects in heterogeneous structure with enhanced crystalline content (regions) leads to slow down charge transport and hence photovoltaic reaction [162]. Similarly, highly sulfonated SPU-DDA also showed negatively deviated current density with low open circuit potential in SGO coated photoanode sensitized device. However, PANi coated photoanode sensitized device improves the performance and stabilize the saturation current density. Consequently, efficiency shifted to little higher values as compared to SGO coated QDSS cell. Thus, highly functionalized polyurethane ionomer increases the number density of ionomeric content in polymer chain which tends to destabilize the gel structure and converted into liquid type behaviour (liquid electrolyte) which is attributed to more hydrophilic content in polyurethane chain. The transition of gel to liquid state can degraded the performance and hence strongly penetrates to the nanoporous photoanode causing high charge recombination. As a result, saturation current density decreases sharply. Oxidized holes are accumulated at the interface of photoanode/ ionomer electrolyte which may leads to photo degradation of QDs layer.

Moreover, ionic aggregation reduces the surface area of pendant group leading to degradation of photovoltaic performance.

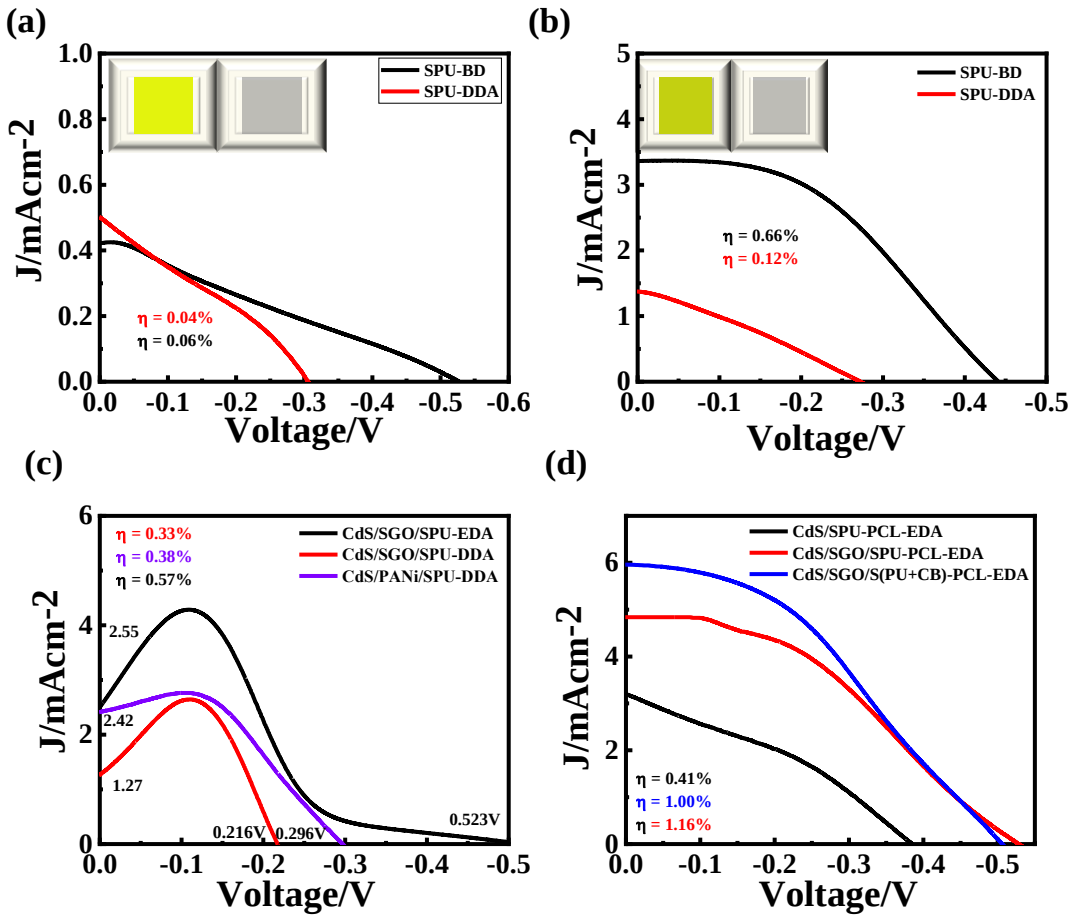

Figure 4.11: (a) Photovoltaic curves of QDSS cells using SPU-BD and SPU-DDA with direct free interface of photoanode/counter electrode. (b) Photovoltaic curves of QDSS cells using SPU-BD and SPU-DDA at the interface doped photoanode/counter electrode.(c) Influence on photovoltaic curves of QDSS cells using SPU-EDA and SPU-DDA at different interface of photoanode/counter electrode. (d) Photovoltaic curves of QDSS cells using SPU-PCL-EDA and composite S (PU+CB)-PCL-EDA at different interfaces of photoanode/counter electrode. Each ionomer gel consists of 20% (w/v).

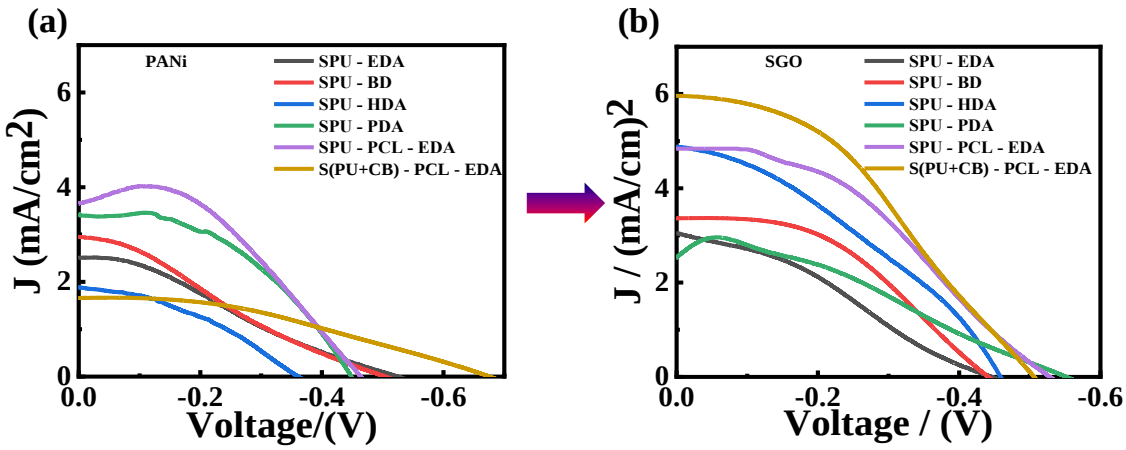

Figure 4.12: J-V characteristic curve of QDSS cells with Variation of chain structure in ionomer electrolyte and photovoltaic reaction under ionomer gel having concentration 20%(w/v) (a) PANi coated photoanode (FTO/TiO_2/CdS/PANi) (b) SGO coated photoanode FTO/TiO_2/CdS/SGO

FTO/TiO_2/MPA-CdS/PANi/SPU/Pt/FTO				
Ionomer electrolyte matrix	**J_{SC}(mA/cm^2)**	**V_{OC}(V)**	**FF**	**η(%)**
SPU-HDA	1.88	0.36	0.38	0.26
SPU-EDA	2.49	0.52	0.28	0.36
SPU-BD	2.93	0.50	0.25	0.37
S(PU+CB)-PCL-EDA	1.65	0.68	0.38	0.42
SPU-PDA	3.19	0.45	0.49	0.70
SPU-PCL-EDA	3.66	0.46	0.46	0.77

Table 4.4: Photovoltaic characteristics of QDSS cells fabricated with PANi coated photoanode (FTO/TiO_2/MPA-CdS/PANi) and ionomer gel matrix with different electrolyte structure (sulfonated polyurethane ionomers)

FTO/TiO_2/MPA-CdS/SGO/SPU/Pt/FTO				
Ionomer electrolyte matrix	**J_{SC}(mA/cm^2)**	**V_{OC}(V)**	**FF**	**η(%)**
SPU-EDA	3.05	0.45	0.31	0.43
SPU-PDA	2.52	0.55	0.38	0.53
SPU-BD	3.39	0.44	0.44	0.65
SPU-HDA	4.87	0.46	0.35	0.78
SPUI-PCL-EDA	4.80	0.53	0.39	1.00
S(PU+CB)-PCL-EDA	5.95	0.51	0.38	1.16

Table 4.5: Photovoltaic characteristic measurements of QDSS cells fabricated with SGO coated photoanode (FTO/TiO_2/MPA-CdS) and ionomer gel matrix with different electrolyte structure (sulfonated polyurethanes).

Photovoltaic reaction has been realized with SPU-PCL-EDA ionomer gel with non coated photoanode CdS sensitized device. The device showed better solar characteristic

curve with photovoltaic properties (J_{SC} = 3.17 mA/cm^2, V_{OC} = 0.38V; η = 0.41%). However, V_{OC} is low which may be due to downward shifting of E_{CB} of Ti – nanooxide leading to enhancement of photocurrent density. Moreover, 20 % (w/v) SPU-PCL-EDA ionomer gel showed better photovoltaic properties (J_{SC} = 4.84 mA/cm^2, V_{OC} = 0.53V; η = 1%) with SGO coated photoanode sensitized device. The photocurrent density and open circuit potential were observed to be improved as compared to values obtained in non surface treated QDSS cell. The high performance is ascribed with electrolyte multiple oxygenic functionalities which interact synergistically with photoanode causing prevention of back reaction during photovoltaic reaction [172]. On other hand, composite ionomer S (PU+CB)-PCL-EDA exhibited better photovoltaic performance (J_{SC} = 5.95 mA/cm^2, V_{OC} = 0.51V; η =1.16%) with SGO coated photoanode sensitized device due to improved interfacial electrical conductivity [156]. The adsorption of Carbon black lowers the surface energy of redox active ionomer content in ionomer electrolyte and thus, facilitates photovoltaic reaction. The interconnected conducting Nano channel intensifies the reversible function of electrolyte [173]. The optimized solar characteristic curves have been shown in **Figure 4.10a, b** with 20% (w/v) ionomer gel electrolyte. The photovoltaic properties have been tuned and values are shown in **Table 4.4** and **Table 4.5.** Finally, it can be concluded that ionomer electrolyte realized the photovoltaic reaction in QDSS cell. The redox active ionic pendant group has been preferred due to structural stabilization efficiency of polyurethane ionomers electrolyte. The functional groups played important role in ionomer electrolyte for improving solar characteristic features [174,175]. 20% (w/v) ionomer gel showed better performance with CdS QDs sensitized solar cell due to improved interfacial electrical properties.

4.8. Conclusions

In summary, redox active functionalized hard segment contents have been developed via incorporation of various diamine/diol chain extenders in polyurethane ionomer chain. The

soft segment content has been modified via PCL-diol to create oxygenic rich center in polyurethane ionomer chain. Redox properties have been realized in free structure of polyurethane ionomers. The differences in electrolyte activity and hence quantum dot sensitized photovoltaic performances have been realized with size and structure difference into polyurethane ionomers. However, the composite ionomer has been created via adsorption of carbon black on sulfonated polyurethane chain. The carbon black lowers the surface energy and intensifies electrical conductivity due to formation of interconnected conducting nanochannel on the surface of ionomer. The conducting pathways with interconnected CB species catalyzed reduction reaction from oxidized ionomer to re-active (native) ionomer and therefore shorten charge-transfer length. Enhanced photovoltaic effect is due to the excellent electrical properties and the huge electro catalytic area of CB in inter-surface area of ionomer gel electrolyte. The maximum power conversion efficiency was observed as 1.16% via electrolyte activity and engineering of polyurethane ionomer.